Ligand Loop Effects on the Free Energy Change of Redox and pH-Dependent Equilibria in Cupredoxins Probed on Amicyanin Variants[†]

Gianantonio Battistuzzi,[‡] Marco Borsari,[‡] Gerard W. Canters,[§] Giulia di Rocco,[‡] Ellen de Waal,[§] Yvonne Arendsen,[§] Alan Leonardi,[‡] Antonio Ranieri,[‡] and Marco Sola*,[‡]

Department of Chemistry and SCS Center, University of Modena and Reggio Emilia, Via Campi 183, 41100 Modena, Italy, and Leiden Institute of Chemistry, Gorlaeus Laboratories, Leiden University, Einsteinweg 55, P.O. Box 9502, 2300 RA Leiden, The Netherlands

ABSTRACT: In this work, we have determined the thermodynamic parameters of the reduction of four different variants of *Thiobacillus versutus* amicyanin by electrochemical techniques. In addition, the thermodynamic parameters were determined of the low-pH conformational change involving protonation of the C-terminal histidine ligand and the concomitant dissociation of this histidine from the Cu(I) ion. In these variants, the native C-terminal loop containing the Cys, His, and Met copper ligands has been replaced with the corresponding polypeptide segments of *Pseudomonas aeruginosa* azurin, *Populus nigra* plastocyanin, *Alcaligenes faecalis* S-6 pseudoazurin, and *Thiobacillus ferrooxidans* rusticyanin. For the reduction reaction, each loop invariably holds an entropic "memory" of the mother protein. The thermodynamics of the low-pH transition vary in a fashion that is species-dependent. When present, the memory effect again shows a large entropic component. In particular, loop elongation tends to favor the formation of the Cu(I)−His bond (hence disfavors His protonation, yielding lower pK_a values) probably due to an increased flexibility of the loop in the reduced state. Overall, it appears that both reduction and low-pH transition are loop-responsive processes. The spacing between the ligands mostly affects the change in the conformational freedom that accompanies the reaction.

The investigation of the reduction reaction of electron transport (ET)[1] metalloproteins may help in understanding the molecular features that determine the reduction potential of the metal center. The latter is a key parameter for protein function (*1−5*). It can be dramatically affected by pH-dependent conformational transitions, which may bear on the electron donor and acceptor capability of the protein (*6−17*). Such a pH-induced transition, thus, may act as a molecular switch of redox activity.

Blue copper proteins (cupredoxins), which participate in respiratory, anabolic, and catabolic processes in plants and bacteria (*1, 7, 18−20*), constitute a protein class for which the redox thermodynamics have been investigated in some detail. In fact, much theoretical and experimental work is available on how the $E°'$ of the copper center in these species and its enthalpic and entropic components are modulated by metal−ligand binding effects and by electrostatic interactions involving permanent and induced protein dipoles, net protein charges, and solvent dipoles (*21−39*). Moreover, many reduced cupredoxins undergo a conformational transition at low pH in which the coordination geometry of the Cu(I) ion changes from distorted tetrahedral to trigonal planar as a consequence of protonation and detachment from the metal of the solvent-exposed histidine ligand (*6−13, 40, 41*). Such a conformational change induces a remarkable increase in the $E°'$ value, because of the stabilization of the cuprous ion in the tricoordinate state, which hampers ET to the physiological partners (*1, 8−10, 12, 13, 24, 38, 39, 41−45*). It has been proposed that this transition may function as a molecular on−off switch of the photosynthetic process (*9, 10, 45−47*). The structural, kinetic, and thermodynamic aspects of this transition (herein termed the "acid" transition) have been thoroughly investigated (*6, 9−13, 40−49*).

We have previously shown that the thermodynamics of both the reduction reaction and the acid transition in cupredoxins are *dominated* by solvent reorganization effects related to the change in the hydrogen bonding network among the water molecules within the hydration sphere of the molecule (*12, 13, 23, 27, 50*). This conclusion relies on the observation that for the cupredoxin family the measured enthalpies and entropies of both reactions show a compensatory behavior; i.e., the mutual differences in the reaction enthalpy and entropy are much greater than those in the reaction free energy (*12, 13, 23, 27, 50−58*). Amicyanin

* To whom correspondence should be addressed. Telephone: +39 059 2055037. Fax: +39 059 373543. E-mail: sola.marco@unimore.it.
[‡] University of Modena and Reggio Emilia.
[§] Leiden University.

[1] Abbreviations: $\Delta H°'_{rc}$, enthalpy change for reduction; $\Delta S°'_{rc}$, entropy change for reduction; $\Delta H°'_{AT}$, enthalpy change for the acid transition; $\Delta S°'_{AT}$, entropy change for the acid transition; $E°'$, standard reduction potential; ET, electron transport; CV, cyclic voltammetry; PGE, pyrolytic graphite edge electrode; SCE, saturated calomel electrode; SHE, standard hydrogen electrode; Ami-Az, Ami-Pc, Ami-PAz, and Ami-Rc, *T. versutus* amicyanin C-terminal loop mutants containing the peptide segments of *P. aeruginosa* azurin (Az), *P. nigra* plastocyanin (Pc), *A. faecalis* S-6 pseudoazurin (PAz), and *T. ferrooxidans* rusticyanin (Rc), respectively.

protein	Sequence of the C-terminal loop										
Amicyanin	**Cys**	Thr		Pro		**His**	Pro				Phe	**Met**
Plastocyanin	**Cys**	Ser		Pro		**His**	Gln	Gly	Ala		Gly	**Met**
Pseudoazurin	**Cys**	Thr		Pro		**His**	Tyr	Ala	Met		Gly	**Met**
Azurin	**Cys**	Thr	Phe	Pro	Gly	**His**	Ser			Ala	Leu	**Met**
Rusticyanin	**Cys**	Gln	Ile	Pro	Gly	**His**	Ala	Ala	Thr		Gly	**Met**

FIGURE 1: Polypeptide sequence of the C-terminal ligand loop in the cupredoxins under investigation.

constitutes an interesting case. It features reaction thermodynamics which nicely fit within the compensation plot for the reduction reaction but not within that for the acid transition (*12*). The latter behavior is due to some yet unknown property of the protein matrix which makes His protonation and detachment from the Cu(I) ion in amicyanin the most favored among cupredoxins (*9, 12, 44, 45*). Here, we have focused on the sequence features of the C-terminal ligand loop containing the three copper ligands Cys, His, and Met. In particular, we have measured the thermodynamics of the reduction reaction and of the low-pH conformational change for four different variants of *Thiobacillus versutus* amicyanin in which the native loop has been replaced with the corresponding polypeptide segments of *Pseudomonas aeruginosa* azurin (Ami-Az), *Populus nigra* plastocyanin (Ami-Pc), *Alcaligenes faecalis* S-6 pseudoazurin (Ami-PAz), and *Thiobacillus ferrooxidans* rusticyanin (Ami-Rc) (*59–61*), which are from two to four residues longer (Figure 1) (*59–61*). The role of the length of the polypeptide spacers among the copper ligands in the thermodynamics of the two processes, namely, on $E^{\circ\prime}$ and the pK_a of the acid transition, has not yet been fully assessed (*59–63*). Evaluation of the influence of loop elongation on the enthalpic and entropic terms may help to distinguish the electronic (ligand binding) and electrostatic effects from those related to the flexibility and solvent accessibility of the metal center.

EXPERIMENTAL PROCEDURES

Proteins. The C-terminal loop mutants of *T. versutus* amicyanin (Ami-Az, Ami-Pc, Ami-PAz, and Ami-Rc) were isolated as reported previously (*59, 61*). All chemicals were reagent grade and were used without further purification. Deionized water (resistivity of 18 MΩ cm^{-1}) was used throughout.

Electrochemical Measurements. Cyclic voltammetry experiments (CV) were carried out with a PAR model 273A potentiostat/galvanostat. A 1 mm diameter pyrolitic graphite disk (PGE) was used as a working electrode for Ami-Az, Ami-Pc, and Ami-PAz (*59*), whereas a mercaptopyridine-treated 2 mm diameter gold disk was used for Ami-Rc (*61*). A saturated calomel electrode and a 5 mm diameter Pt electrode served as the reference and counter electrode, respectively. The modification of the working electrode, the configuration of the "non-isothermal" cell (*64–66*) used for the thermodynamic measurements, the properties of the voltammetric signal, and the other experimental details of the *T*-dependent and pH-dependent E° measurements were reported previously (*12, 13, 21, 25–27*).

Thermodynamic Parameters. Using a non-isothermal cell, the entropy for reduction of the oxidized proteins ($\Delta S^{\circ\prime}_{rc}$) is given by (*22, 64–66*)

$$\Delta S^{\circ\prime}_{rc} = S^{\circ\prime}_{red} - S^{\circ\prime}_{ox} = nF(dE^{\circ\prime}/dT)$$

Thus, $\Delta S^{\circ\prime}_{rc}$ was determined from the slope of the plot of $E^{\circ\prime}$ versus temperature which turns out to be linear under the hypothesis that $\Delta S^{\circ\prime}_{rc}$ is constant over the limited temperature range that was investigated. With the same assumption, the enthalpy change ($\Delta H^{\circ\prime}_{rc}$) was obtained from the Gibbs−Helmholtz equation, namely, from the slope of the $E^{\circ\prime}/T$ versus $1/T$ plot (*21, 24−27*).

The thermodynamic parameters for the acid transition ($\Delta H^{\circ\prime}_{AT}$ and $\Delta S^{\circ\prime}_{AT}$) were determined from the *T* dependence of the (apparent) pK_a values obtained from the pH dependence of the reduction potential, as described elsewhere (*7, 8, 10, 12, 13, 24, 38, 39, 42−45, 59, 61, 67*). For all species but Ami-Rc, the $E^{\circ\prime}$ increases linearly below pH 6, with a slope of approximately 50−60 mV/pH (not shown) as a result of the coupling of Cu^{2+} reduction with the protonation of the C-terminal His residue, and the concomitant detachment from the metal. Ami-Rc is affected by a severe peak broadening that prevents determination of $E^{\circ\prime}$ below pH 6, in agreement with a previous report (*61*). The low-pH region of the $E^{\circ\prime}$/pH profiles was fitted to the following single acid−base equilibrium equation, which applies to the above conditions (*7, 12, 13, 67*):

$$E^{\circ\prime} = E^{\circ\prime}_{lim} + 2.3\frac{RT}{F}\log(1 + [H^+]/K_a) \quad (1)$$

where $E^{\circ\prime}_{lim}$ is the limiting $E^{\circ\prime}$ value at high pH and K_a is the (apparent, since it is measured at finite ionic strength) His proton dissociation constant for the reduced protein. Because of the deterioration of the voltammetric signals at low pH, measurements could not be performed below pH 3. The pK_a values were determined at different temperatures in the range of 5−35 °C. The transition thermodynamics have been evaluated using the integrated van't Hoff equation (*12, 13, 16, 17*):

$$pK_{app} = \frac{\Delta H^{\circ\prime}_{AT}}{2.3R}\frac{1}{T} - \frac{\Delta S^{\circ\prime}_{AT}}{2.3R} \quad (2)$$

In particular, the enthalpy and entropy changes were obtained from the slope and intercept of the pK_a versus $1/T$ plot, respectively.

RESULTS AND DISCUSSION

The thermodynamics of $Cu^{2+} \rightarrow Cu^+$ reduction ($\Delta H^{\circ\prime}_{rc}$ and $\Delta S^{\circ\prime}_{rc}$) for the *T. versutus* amicyanin loop mutants, determined from the temperature profiles of $E^{\circ\prime}$ (Figure 2), are listed in Table 1 (the $E^{\circ\prime}/T$ vs $1/T$ plots yielding the $\Delta H^{\circ\prime}_{rc}$ values are available as supporting information). Also listed are the thermodynamic parameters determined previously for the cupredoxins from which the various ligand loops were taken (herein named "donor" cupredoxins) (*21*). The van't Hoff plots for the acid transition (AT) are shown in Figure 3. To facilitate discussion, we refer to the protonation reaction; therefore, the $\Delta H^{\circ\prime}_{AT}$ and $\Delta S^{\circ\prime}_{AT}$ values obtained from the least-squares fits of the pK_a versus $1/T$ plots to eq 2 are listed in Table 2 with the sign changed (*12, 13*). The pK_a value for Ami-Rc, which could not be determined at any temperature due to signal deterioration below pH 6, was estimated by NMR to be lower than 4.5 at 25 °C (*61*).
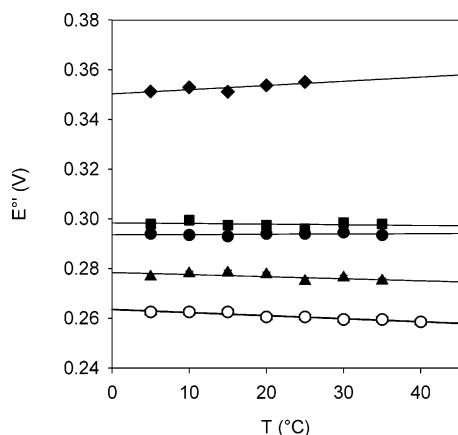
FIGURE 2: Temperature dependence of the reduction potential of *T. versutus* amicyanin loop mutants. The slope of the plots yields the $\Delta S^{\circ\prime}_{rc}$ values: (○) wild-type Ami, (●) Ami-Az, (■) Ami-Pc, (▲) Ami-PAz, and (◆) Ami-Rc. The protein concentration was 0.1 mM, and the base electrolyte was 0.1 M phosphate (pH 7). Solid lines are least-squares fits to the data points. Error bars have the same dimensions as the symbols.

Ligand loop replacement in amicyanin induces measurable changes in the free energy of both reactions in most cases. The $E^{\circ\prime}$ values for the four loop mutants are higher than that of wild-type amicyanin and lower than those of the donor cupredoxins, in agreement with previous reports (*59, 61*). In particular, the $\Delta E^{\circ\prime}$ values ($= E^{\circ\prime}_{mut} - E^{\circ\prime}_{wt-ami}$) increase with increasing reduction potentials of the donor cupredoxins (Table 1) (this observation is merely phenomenological; there is no clear basis on which any quantitative correlation can be discussed). Hence, each inserted loop holds a sort of "memory" of the native donor protein. However, we note that the thermodynamics of the reduction reaction in the loop mutants are much closer to those for wild-type Ami than to those for the native donor species. This would suggest that the structural and dynamic features of the inserted ligand loops are not tightly conserved in the mutants, but are affected by the rigid scaffold of the host protein that tends to reproduce the features of native amicyanin. These results are in line with spectroscopic results for these loop mutants (*49, 59, 61, 68*). The way in which loop elongation affects the pK_a of the acid transition is not unequivocal. In fact, the pK_a values for the Ami-Pc, Ami-PAz, and Ami-Rc mutants are lower than that for wild-type amicyanin, as are those of the donor proteins, but the pK_a value of Ami-Az is almost identical to that of wild-type Ami even though native azurin does not undergo such a transition down to pH 4 (*12, 30, 31, 40, 59, 61*). Therefore, the C-terminal ligand loop affects the redox potential of the loop variants in a generic way, but its effect on the acid transition is less predictable. This means, as noted previously (*59*), that in addition to spacing between the copper ligands, structural features of the loop affect the reactions. The same conclusion was reached by loop contraction experiments (*62, 63*) in which the Ami loop was introduced into Paz, Pc, and Az. In all cases, the effects were the opposite of those discussed here. Loop contraction indeed resulted in a decrease in $E^{\circ\prime}$ by 30–60 mV and in an increase in the pK_a values.

Effects of Loop Substitution on the Reduction Reaction. The mutation-induced changes in the free energy of reduction feature only a modest enthalpic contribution and in most cases are mainly entropic in origin (Table 1). We have previously shown that the main determinants of the enthalpy change of the reduction reaction in blue copper proteins are localized within the first coordination sphere of the metal, and are related, in particular, to the strength of the bond between the Cu and the axial ligand (involving a Met sulfur or a Gln oxygen) (*21, 24, 26, 27*). However, also electrostatic interactions between the metal and permanent and induced dipoles (protein and solvent) and nearby charges on the protein (*21, 24–27, 50*) affect the reduction enthalpy, as previously shown for plastocyanin and azurin mutants and in agreement with theoretical estimates (*35–37, 69–71*). Metal–charge interactions must indeed be invoked to understand the conservation of the reduction enthalpy of amicyanin following loop replacements. In fact, it has been shown previously that rhombic sites (with tetragonal or tetrahedral distortions) enthalpically stabilize the Cu(II) ion more than the axial sites (*21, 24, 26, 27, 38, 39*), most probably because of a stronger axial copper ligation (*21, 24, 26, 27, 38, 39*). Hence, the increase in the rhombicity of the copper site in the loop mutants (*59, 61*) would have been expected to increase $\Delta H^{\circ\prime}_{rc}$ (less negative values) with respect to that of the wild-type protein. Therefore, the invariance of $\Delta H^{\circ\prime}_{rc}$ upon loop replacement may be interpreted as the result of two counteracting effects: enthalpic stabilization of Cu(II) due to the increase in metal site rhombicity and an opposite electrostatic contribution. The latter term is probably related to the greater length of the inserted ligand loops which reduces the solvent accessibility of the redox center and enhances the number of the surrounding protein permanent dipoles in the mutants (*59, 61*). Thus, a more effective screening of the electrostatic interaction between the metal center and the water dipoles is obtained, and a selective enthalpic stabilization of the reduced over the oxidized form is expected, analogous to the behavior of other cupredoxins (*21, 25–27*). This would also be in accordance with recent PDLD/S-LRA calculations (*35*), which indicate that the ligand loops in plastocyanin and rusticyanin increase the reduction potential by ~50 and ~80 mV, respectively, as a consequence of the electrostatic effect of their permanent dipoles.

The changes in the entropy of reduction (and in the entropy of the acid transition as well) are related to changes in the solvation and flexibility of the polypeptide chain (*21, 24–27, 38, 39, 50*). Since the solvent contribution is compensated by the enthalpic term, it cannot be responsible for the entropy-based free energy changes detected for the mutants presented here. Therefore, the dominant contribution must come from the inserted loops, given that the structural features of the rest of the protein are almost unaffected by the loop elongation (*59, 61*). The reduction reaction is entropically more favored in the loop mutants (except for Ami-PAz). This, in agreement with previous suggestions (*59*), can be tentatively ascribed to a reduction-induced increase in the flexibility of the ligand loop in Ami-Az, Ami-Pc, and Ami-Rc as compared to that of the wild-type amicyanin for which the opposite effect (resulting in a negative $\Delta S^{\circ\prime}_{rc}$ value) is apparently prevailing. The reason of this effect is likely to be related to the poorer packing of the non-native loops against the β-barrel structure of the protein as compared to the native loop in amicyanin, as proposed previously by Canters et al. (*59, 61*). However, since the loops include mostly nonpolar residues, the

Table 1: Thermodynamics of the Cu(II) → Cu(I) Reduction for the Loop Mutants of *T. versutus* Amicyanin and for the Wild-Type Proteins[a]

protein	$E^{\circ\prime}$ (mV)	$\Delta H^{\circ\prime}_{rc}$ (kJ/mol)	$\Delta S^{\circ\prime}_{rc}$ (J mol^{-1} K^{-1})	$-\Delta H^{\circ\prime}_{rc}/F$ (mV)	$T\Delta S^{\circ\prime}_{rc}/F$[b] (mV)	$\Delta E^{\circ\prime}$[c] (mV)	$-\Delta\Delta H^{\circ\prime}_{rc}/F$[c] (mV)	$T\Delta\Delta S^{\circ\prime}_{rc}/F$[c] (mV)
wild-type Ami[d]	+255	−29	−12	+301	−37			
Ami-Az[e]	+294	−28	+1	+290	+3	+39	−11	+40
Ami-Pc[e]	+296	−30	−2	+311	−6	+41	+10	+31
Ami-PAz[e]	+275	−30	−13	+311	−40	+20	+10	−3
Ami-Rc[e]	+355	−29	+16	+301	+49	+100	0	+86
P. aeruginosa Az[f]	+307	−49	−65	+508	−201			
Spi Pc[f]	+366	−46	−36	+477	−111			
A. faecalis PAz[d]	+275	−16	+37	+166	+114			
T. ferrooxidans Rc[g]	+680							

[a] All values obtained in 0.1 M phosphate buffer (pH 7). Errors for $\Delta H^{\circ\prime}_{rc}$ and $\Delta S^{\circ\prime}_{rc}$ are ±2 kJ/mol and ±6 J mol^{-1} K^{-1}, respectively (calculated from the upper value of the standard deviation of the least-squares fits of the data points within the series). The sum $-\Delta H^{\circ\prime}_{rc}/F + T\Delta S^{\circ\prime}_{rc}/F$ often does not close exactly to $E^{\circ\prime}$ since, because of the experimental error, the $\Delta H^{\circ\prime}_{rc}$ and $\Delta S^{\circ\prime}_{rc}$ values are rounded to the closest integer. [b] At 25 °C. [c] $\Delta E^{\circ\prime}$ ($=E^{\circ\prime}_{mut} - E^{\circ\prime}_{wt-Ami}$); the same difference holds for the enthalpy and entropy values. [d] From ref 27. [e] From this work. [f] From ref 21. Note that the loops of the plastocyanins from spinach and *P. nigra* are identical. [g] From ref 31.
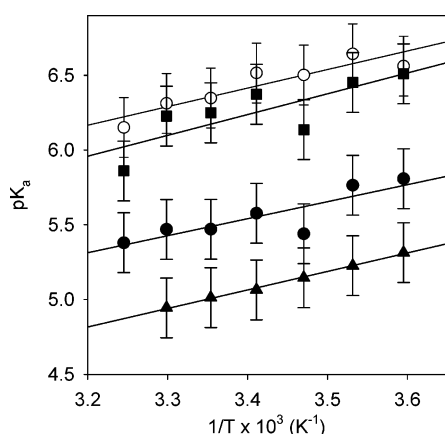

FIGURE 3: van't Hoff plots for the acid transition of loop amicyanin mutants: (○) wild-type Ami, (●) Ami-Az, (■) Ami-Pc, and (▲) Ami-PAz. Solid lines are least-squares fits to the data points. Please note that the transition enthalpies obtained from the slope of these plots refer to the deprotonation reaction; those reported in Table 2 instead refer to the protonation reaction, and hence, the signs are reversed.

Table 2: Thermodynamic Parameters for the Acid Transition (AT) (involving protonation at the metal site) of the Loop Mutants of *T. versutus* Amicyanin[a]

protein	$\Delta H^{\circ\prime}_{AT}$[b] (kJ/mol)	$\Delta S^{\circ\prime}_{AT}$[b] (J mol^{-1} K^{-1})	$-T\Delta S^{\circ\prime}_{AT}$[c] (kJ/mol)	$\Delta G^{\circ\prime}_{AT}$[d] (kJ/mol)	pK_a[c,d]
wild-type Ami[e]	−24	+42	−12	−36	6.4
Ami-Az	−27	+29	−9	−36	6.3
Ami-Pc	−22	+32	−10	−32	5.6
Ami-PAz	−24	+16	−5	−29	5.1
Ami-Rc	na	na	na	na	<4.5[e]
cucumber Pc[f]	−41	−54	+16	−25	4.4
spinach Pc[f]	−47	−77	+23	−24	4.2
Rhus vernicifera Sc[f]	−11	+49	−15	−26	4.5
CBP[f]	+34	+197	−59	−24	4.2

[a] Values obtained in 10 mM phosphate buffer and 100 mM sodium chloride. [b] Errors for $\Delta H^{\circ\prime}_{AT}$ and $\Delta S^{\circ\prime}_{AT}$ values are ±2 kJ/mol and ±6 J mol^{-1} K^{-1}, respectively (calculated from the upper value of the standard deviation of the least-squares fits to the data points within the series). [c] At 298 K. [d] The error affecting the apparent pK_a values is ±0.2 pH unit (determined from the upper value of the standard deviation of the least-squares fits to the data points within the series). As a consequence, the error for $\Delta G^{\circ\prime}_{AT}$ is ±1 kJ/mol. [e] From ref 60. [f] From ref 12.

oxidation state-dependent effect is not easy to explain, although the increased polarity of the non-native loop due to the presence of one more polar residue adjacent to the solvent-exposed His may play a role in sensing the decreased charge of the metal site upon reduction (from +1 to 0).

Effects of Loop Substitution on the Acid Transition. The interplay between transition enthalpy and entropy in the various mutants is different for the acid transition. In Ami-Az, the changes in $\Delta H^{\circ\prime}_{AT}$ and $\Delta S^{\circ\prime}_{AT}$ are compensatory, with the former tending to increase the pK_a. In Ami-Pc, the two effects are small but additive and both decrease the pK_a. In Ami-PAz, the pK_a decrease is totally entropic. Thus, for Ami-Pc, Ami-PAz, and Ami-Rc, elongation of the loop between the His and Met ligands disfavors protonation and dissociation of the His ligand. This effect is remarkable for the latter mutant (*61*). Apparently, the rusticyanin loop contains in itself some remarkable properties that prevent His protonation and let the protein function physiologically at very acidic pH values (*30, 31, 61*). These data support the hypothesis that the acid transition is a sequence-responsive process (*10, 11, 42, 45, 62, 63, 70*) and indicate that the effect of the different lengths of the spacers has an important entropic component. In particular, in all cases, loop elongation apparently tends to favor the formation of the Cu-(I)−His bond (hence yielding lower pK_a values) probably due to an increased flexibility of the loop in the reduced state and a favorable entropic term. This would explain why Ami-Rc, with the longest loop, has the highest $\Delta S^{\circ\prime}_{rc}$ value in the series (Table 1) and displays the lowest pK_a (*61*). The same argument may be used to tentatively explain the variability of the pK_a values for the acid transition in native species.

In this context, the case of Ami-Az is puzzling. The invariance of the free energy is the result of an enthalpic term which favors protonation (i.e., a pK_a increase) and an entropic term which, as for the other species, favors deprotonation. The origin of the enthalpic effect cannot be established safely at present. It may originate from a bonding effect involving the C-terminal His in the new environment provided by the Ami scaffold. The loop replacement also may have an effect on the rotational barriers of His in both the metal-bound and protonated states which have been proposed to strongly influence the pK_a and the kinetics of the transition (*40*).

In conclusion, it appears that a transition-induced change in the number of accessible conformational states (which are sensitive to sequence features) is one of the determinants of the free energy change of the acid transition in blue copper proteins. This change appears to be sensitive to the sequence characteristics of the ligand loop.

SUPPORTING INFORMATION AVAILABLE

$E°'/T$ versus $1/T$ plots of *T. versutus* amicyanin loop mutants (Figure 1) and $E°'/pH$ profiles for the Ami-PAz mutant at differerent temperatures (Figure 2). This material is available free of charge via the Internet at http://pubs.acs.org.

REFERENCES

1. Gray, H. B., and Ellis, W. R., Jr. (1994) Electron Transfers in Biology, in *Bioinorganic Chemistry* (Bertini, I., Gray, H. B., Lippard, S. J., and Valentine, J. S., Eds.) pp 315−364, University Science Books, Sausalito, CA.
2. Gray, H. B., and Winkler, J. R. (2003) Electron tunneling through proteins, *Q. Rev. Biophys. 36*, 341−372.
3. Rao, P. V., and Holm, R. H. (2004) Synthetic Analogues of the Active Sites of Iron−Sulfur Proteins, *Chem. Rev. 104*, 527−560.
4. Reedy, C. J., and Gibney, B. R. (2004) Heme Protein Assemblies, *Chem. Rev. 104*, 617−650.
5. Rorabacher, D. B. (2004) Electron Transfer by Copper Centers, *Chem. Rev. 104*, 651−697.
6. Guss, J. M., Harrowell, P. R., Murata, M., Norris, V. A., and Freeman, H. C. (1986) Crystal structure analyses of reduced (Cu I) poplar plastocyanin at six pH values, *J. Mol. Biol. 192*, 361−387.
7. Sykes, A. G. (1991) Active-Site Properties of the Blue Copper Proteins, *Adv. Inorg. Chem. 36*, 377−408.
8. Niles McLeod, D. D., Freeman, H. C., Harvey, I., Lay, P. A., and Bond, A. M. (1996) Voltammetry of Plastocyanin at a Graphite Electrode: Effects of Structure, Charge, and Electrolyte, *Inorg. Chem. 35*, 7156−7165.
9. Zhu, Z., Cunane, L. M., Chen, Z. W., Durley, R. C. E., Mathews, F. S., and Davidson, V. L. (1998) Molecular basis for interprotein complex-dependent effects on the redox properties of amicyanin, *Biochemistry 37*, 17128−17136.
10. Dennison, C., Lawler, A. T., and Kohzuma, T. (2002) Unusual properties of plastocyanin from the fern *Dryopteris* crassirhizoma, *Biochemistry 41*, 552−560.
11. Sato, K., Kohzuma, T., and Dennison, C. (2003) Active-site structure and electron-transfer reactivity of plastocyanins, *J. Am. Chem. Soc. 125*, 2101−2112.
12. Battistuzzi, G., Borsari, M., Canters, G. W., de Waal, E., Leonardi, A., Ranieri, A., and Sola, M. (2002) Thermodynamics of the Acid Transition in Blue Copper Proteins, *Biochemistry 41*, 14293−14298.
13. Battistuzzi, G., Borsari, M., Di Rocco, G., Leonardi, A., Ranieri, A., and Sola, M. (2005) *ChemBioChem 6*, 692−696.
14. Wilson, M. T., and Greenwood, C. (1996) The alkaline transition in ferricytochrome *c*, in *Cytochrome c: A Multidisciplinary Approach* (Scott, R. A., and Mauk, A. G., Eds.) pp 611−634, University Science Books, Sausalito, CA.
15. Döppner, S., Hildebrandt, P., Rosell, F. I., and Mauk, A. G. (1998) Alkaline Conformational Transitions of Ferricytochrome *c* Studied by Resonance Raman Spectroscopy, *J. Am. Chem. Soc. 120*, 11246−11255.
16. Battistuzzi, G., Borsari, M., Loschi, L., Martinelli, A., and Sola, M. (1999) Thermodynamics of the Alkaline Transition of Cytochrome *c*, *Biochemistry 38*, 7900−7907.
17. Battistuzzi, G., Borsari, M., Ranieri, A., and Sola, M. (2002) Conservation of the free energy change of the alkaline isomerization in mitochondrial and bacterial cytochromes *c*, *Arch. Bioch. Biophys. 404*, 227−233.
18. Farver, O., and Pecht, I. (1994) in *Copper Proteins and Copper Enzymes* (Lontie, R., Ed.) Vol. 1, pp 183−214, CRC Press, Boca Raton, FL.
19. Farver, O. (1996) Copper proteins, in *Protein Electron Transfer* (Bendall, D. S., Ed.) pp 161−188, Bios, Oxford, U.K.
20. Messerschmidt, A. (1998) Metal sites in small blue copper proteins, blue copper oxidases and vanadium-containing enzymes, *Struct. Bonding 90*, 37−68.
21. Battistuzzi, G., Borsari, M., Loschi, L., Righi, F., and Sola, M. (1999) Redox thermodynamics of blue copper proteins, *J. Am. Chem. Soc. 121*, 501−506.
22. Taniguchi, V. T., Sailasuta-Scott, N., Anson, F. C., and Gray, H. B. (1980) Thermodynamics of metalloprotein electron transfer reactions, *Pure Appl. Chem. 52*, 2275−2281.
23. Canters, G. W., Kolczak, U., Armstrong, F. A., Jeuken, L. J. C., Camba, R., and Sola, M. (2000) The effect of pH and ligand exchange on the redox properties of blue copper proteins, *Faraday Discuss. 116*, 205−220.
24. Battistuzzi, G., Borsari, M., Loschi, L., and Sola, M. (1997) Redox thermodynamics, acid−base equilibria and salt-induced effects for the cucumber basic protein. General implications for blue-copper proteins, *J. Biol. Inorg. Chem. 2*, 350−359.
25. Battistuzzi, G., Borsari, M., Loschi, L., Menziani, M. C., De Rienzo, F., and Sola, M. (2001) Control of Metalloprotein Reduction Potential: The Role of Electrostatic and Solvation Effects Probed on Plastocyanin Mutants, *Biochemistry 40*, 6422−6430.
26. Battistuzzi, G., Borsari, M., Canters, G. W., de Waal, E., Loschi, L., Warmerdam, G., and Sola, M. (2001) Enthalpic and Entropic Contributions to the Mutational Changes in the Reduction Potential of Azurin, *Biochemistry 40*, 6707−6712.
27. Battistuzzi, G., Bellei, M., Borsari, M., Canters, G. W., de Waal, E., Jeuken, L. J. C., Ranieri, A., and Sola, M. (2003) Control of Metalloprotein Reduction Potential: Compensation Phenomena in the Reduction Thermodynamics of Blue Copper Proteins, *Biochemistry 42*, 9214−9220.
28. George, S. D., Basumallick, L., Szilagy, R. K., Randall, d. W., Hill, M. G., Nersissian, A. M., Valentine, J. S., Hedman, B., Hodgson, K. O., and Solomon, E. I. (2003) Spectroscopic Investigation of Stellacyanin Mutants: Axial Ligand Interactions at the Blue Copper Site, *J. Am. Chem. Soc. 125*, 11314−11328.
29. Berry, S. M., Ralle, M., Low, D. W., Blackburn, N. J., and Lu, Y. (2003) Probing the role of axial methionine in the blue copper center of azurin with unnatural amino acids, *J. Am. Chem. Soc. 125*, 8760−8768.
30. Hall, J. F., Kanbi, L. D., Strange, R. W., and Hasnain, S. S. (1999) Role of the axial ligand in type 1 Cu centers studied by point mutations of Met148 in rusticyanin, *Biochemistry 38*, 12675−12680.
31. Hall, J. F., Kanbi, L. D., Harvey, I., Murphy, L. M., and Hasnain, S. S. (1998) Modulating the redox potential and acid stability of rusticyanin by site-directed mutagenesis of Ser86, *Biochemistry 37*, 11451−11458.
32. Libeu, C. A. P., Kukimoto, M., Nishiyama, M., Horinouchi, S., and Adman, E. T. (1997) Site-directed mutants of pseudoazurin: Explanation of increased redox potentials from X-ray structures and from calculation of redox potential differences, *Biochemistry 36*, 13160−13179.
33. Botuyan, M. V., Toy Palmer, A., Chung, B., Blake, R. C., Beroza, P., Case, D. A., and Dyson, H. J. (1996) NMR solution structure of Cu(I) rusticyanin from *Thiobacillus ferrooxidans*: Structural basis for the extreme acid stability and redox potential, *J. Mol. Biol. 263*, 752−767.
34. Ryde, U., Olsson, M. H. M., Roos, B. O., De Kerpel, J. O. A., and Pierloot, K. (2000) On the role of strain in blue copper proteins, *J. Biol. Inorg. Chem. 5*, 565−574.
35. Olsson, M. H. S., Gong, G., and Warshel, A. (2003) Frozen Density Functional Free Energy Simulations of Redox Proteins: Computational Studies of the Reduction Potential of Plastocyanin and Rusticyanin, *J. Am. Chem. Soc. 125*, 5025−5039.
36. Li, H., Webb, S. P., Ivanic, J., and Jensen, J. H. (2004) Determinants of the Relative Reduction Potentials of Type-1 Copper Sites in Proteins, *J. Am. Chem. Soc. 126*, 8010−8019.
37. Datta, S. N., Sudhamsu, J., and Pandey, A. (2004) Theoretical determination of the standard reduction potential of plastocyanin in vitro, *J. Phys. Chem. B 108*, 8007−8016.
38. Battistuzzi, G., Borsari, M., Loschi, L., and Sola, M. (1998) Redox properties of the basic blue protein (plantacyanin) from spinach, *J. Inorg. Biochem. 69*, 97−100.
39. Battistuzzi, G., Borsari, M., Loschi, L., Ranieri, A., Sola, M., Mondovì, B., and Marchesini, A. (2001) *J. Inorg. Biochem. 83*, 223−227.
40. Buning, C., and Comba, P. (2000) Protonation of the copper(I) form of the blue copper proteins plastocyanin and amicyanin: A molecular dynamics study, *Eur. J. Inorg. Chem.*, 1267−1273.
41. Vakoufari, E., Wilson, K. S., and Petratos, K. (1994) The crystal structures of reduced pseudoazurin from *Alcaligenes faecalis* S-6 at two pH values, *FEBS Lett. 347*, 203−206.
42. Dennison, C., Kohzuma, T., McFarlane, W., Suzuki, S., and Sykes, A. G. (1994) Reversible active site protonation and electron-transfer properties of *Achromobacter cycloclastes* pseudoazurin: Comparisons with other type 1 copper proteins, *J. Chem. Soc., Chem. Commun.*, 581−582.

43. Kohzuma, T., Dennison, C., McFarlane, W., Nakashima, S., Kitagawa, T., Inoue, T., Kai, Y., Nishio, N., Shidara, S., Suzuki, S., and Sykes, A. G. (1995) Spectroscopic and electrochemical studies on active site transitions of the type 1 copper protein pseudoazurin from *Achromobacter cycloclastes*, *J. Biol. Chem. 43*, 25733−25738.

44. Machczynski, C. M., Gray, H. B., and Richards, J. H. (2002) An outer-sphere hydrogen-bond network constrains copper coordination in blue proteins, *J. Inorg. Biochem. 88*, 375−380.

45. Yanagisawa, S., Sato, K., Kikuchi, M., Kohzuma, T., and Dennison, C. (2003) Introduction of a p−p Interaction at the Active Site of a Cupredoxin: Characterization of the Met16Phe Pseudoazurin Mutant, *Biochemistry 42*, 6853−6862.

46. Jeuken, L. J. C., Ubbink, M., Bitter, J. H., van Vliet, P., Meyer-Klaucke, W., and Canters, G. W. (2000) The Structural Role of the Copper-coordinating and Surface-exposed Histidine Residue in the Blue Copper Protein Azurin, *J. Mol. Biol. 299*, 737−755.

47. Freeman, H. C. (1981) Electron transfer in 'blue' copper proteins, *Coord. Chem. 21*, 29−51.

48. Lommen, A., and Canters, G. W. (1990) pH-dependent redox activity and fluxionality of the copper site in amicyanin from *Thiobacillus yersutus* as studied by 300- and 600-MHz ^{1}H NMR, *J. Biol. Chem. 265*, 2768−2774.

49. Dennison, C., Vijgenboom, E., Hagen, W. R., and Canters, G. W. (1996) Loop-directed mutagenesis converts amicyanin from *Thiobacillus versutus* into a novel blue copper protein, *J. Am. Chem. Soc. 118*, 7406−7407.

50. Battistuzzi, G., Borsari, M., Di Rocco, G., Ranieri, A., and Sola, M. (2004) Enthalpy/entropy compensation phenomena in the reduction thermodynamics of electron transport metalloproteins, *J. Biol. Inorg. Chem. 9*, 23−26.

51. Lumry, R., and Rajender, S. (1970) Enthalpy−entropy compensation phenomena in water solutions of proteins and small molecules: A ubiquitous property of water, *Biopolymers 9*, 1125−1227.

52. Grunwald, E., and Steel, C. (1995) Solvent Reorganization and Thermodynamic Enthalpy−Entropy Compensation, *J. Am. Chem. Soc. 117*, 5687−5692.

53. Lumry, R. (1971) *Electron and Coupled Energy Transfer in Biological Systems*, Marcel Dekker, New York.

54. Grunwald, E. (1986) Thermodynamic properties of nonpolar solutes in water and the structure of hydrophobic hydration shells, *J. Am. Chem. Soc. 108*, 5726−5731.

55. Liu, L., and Guo, Q.-X. (2001) Isokinetic relationship, isoequilibrium relationship, and enthalpy−entropy compensation, *Chem. Rev. 101*, 673−695.

56. Liu, L., Yang, C., and Guo, Q.-X. (2000) A study on the enthalpy−entropy compensation in protein unfolding, *Biophys. Chem. 84*, 239−251.

57. Ben-Naim, A. (1975) Hydrophobic interaction and structural changes in the solvent, *Biopolymers 14*, 1337−1355.

58. Lee, B., and Graziano, G. (1996) A Two-State Model of Hydrophobic Hydration That Produces Compensating Enthalpy and Entropy Changes, *J. Am. Chem. Soc. 118*, 5163−5168.

59. Buning, C., Canters, G. W., Comba, P., Dennison, C., Jeuken, L., Melter, M., and Sanders-Loehr, J. (2000) Loop-Directed Mutagenesis of the Blue Copper Protein Amicyanin from *Paracoccus versutus* and Its Effect on the Structure and the Activity of the Type-1 Copper Site, *J. Am. Chem. Soc. 122*, 204−211.

60. Kalverda, A. P., Salgado, J., Dennison, C., and Canters, G. W. (1996) Analysis of the Paramagnetic Copper(II) Site of Amicyanin by ^{1}H NMR Spectroscopy, *Biochemistry 35*, 3085−3092.

61. Remenyi, R., Jeuken, L. J. C., Comba, P., and Canters, G. W. (2001) An amicyanin C-terminal loop mutant where the active-site histidine donor cannot be protonated, *J. Biol. Inorg. Chem. 6*, 23−26.

62. Yanagisawa, S., and Dennison, C. (2003) Loop-Contraction Mutagenesis of a Type 1 Copper Site, *J. Am. Chem. Soc. 125*, 4974−4975.

63. Yanagisawa, S., and Dennison, C. (2004) Loop-Contraction Mutagenesis of Type 1 Copper Sites, *J. Am. Chem. Soc. 126*, 15711−15719.

64. Yee, E. L., Cave, R. J., Guyer, K. L., Tyma, P. D., and Weaver, M. J. (1979) A survey of ligand effects upon the reaction entropies of some transition metal redox couples, *J. Am. Chem. Soc. 101*, 1131−1137.

65. Yee, E. L., and Weaver, M. J. (1980) Functional dependence upon ligand composition of the reaction entropies for some transition-metal redox couples containing mixed ligands, *Inorg. Chem. 19*, 1077−1079.

66. Koller, K. B., and Hawkridge, F. M. (1985) Temperature and electrolyte effects on the electron-transfer reactions of cytochrome *c*, *J. Am. Chem. Soc. 107*, 7412−7417.

67. Illerhaus, J., Altshmied, L., Reichert, J., Zak, E., Herrmann, R. G., and Haelhnel, W. (2000) Dynamic interaction of plastocyanin with the cytochrome bf complex, *J. Biol. Chem. 275*, 17590−17595.

68. Canters, G. W., unpublished data.

69. Susuki, S., Sakurai, T., Shidara, S., and Iwasaki, H. (1989) Spectroscopic characterization of cobalt(II)-substituted *Achromobacter* pseudoazurin: Similarity of the metal center in Co(II)-pseudoazurin to those in Co(II)-plastocyanin and Co(II)-plantacyanin, *Inorg. Chem. 28*, 802−804.

70. Durley, R., Chen, L., Louis, L. W., Mathews, F. S., and Davidson, V. L. (1993) Crystal structure analysis of amicyanin and apoamicyanin from *Paracoccus denitrificans* at 2.0 and 1.8 Å resolution, *Protein Sci. 2*, 739−752.

71. Warshel, A., Papazyan, A., and Muegge, I. (1997) Microscopic and semimacroscopic redox calculations: What can and cannot be learned from continuum models, *J. Biol. Inorg. Chem. 2*, 143−152.